Journal of
Mechanics of
Materials and Structures

EFFECT OF NUMBER OF CROWNS ON THE CRUSH RESISTANCE IN OPEN-CELL STENT DESIGN

Gideon Praveen Kumar, Keping Zuo, Li Buay Koh, Chi Wei Ong, Yucheng Zhong,
Hwa Liang Leo, Pei Ho and Fangsen Cui

Volume 15, No. 1 January 2020

msp

JOURNAL OF MECHANICS OF MATERIALS AND STRUCTURES
Vol. 15, No. 1, 2020
dx.doi.org/10.2140/jomms.2020.15.75

EFFECT OF NUMBER OF CROWNS ON THE CRUSH RESISTANCE IN OPEN-CELL STENT DESIGN

GIDEON PRAVEEN KUMAR, KEPING ZUO, LI BUAY KOH, CHI WEI ONG, YUCHENG ZHONG, HWA LIANG LEO, PEI HO AND FANGSEN CUI

Our group is developing novel preferential covered carotid stents aimed at preventing friable parts from atherosclerotic plaques from dislodging into the cerebral blood flow, and also preserving external carotid artery (ECA) perfusion through slits on the membrane. Enhanced ECA flow rates can be achieved by designing bare metal stents with larger cells that can accommodate more slits for enhanced blood flow to the ECA where the stents have fewer crowns in the circumferential direction. The general perception is that the stent stiffness and thereby the crush resistance will decrease with fewer crowns in the circumferential direction. However, we observed the opposite effect. To study the effect of crown number on crush resistance of stents, finite element analysis (FEA) was used to evaluate the crush resistance of open-cell stent designs by varying the number of crowns. From FEA simulation results, it was found that the crush resistance of the open-cell stent design actually increases with fewer crowns. To verify this effect, three stent designs with different crown numbers were fabricated and subjected to crush resistance experimental testing. The experimental testing further confirmed the effect observed by FEA. Finally, a simplified analytical model was proposed to explain why the crush resistance of stent increases with a reduction in the number of stent crowns. From this study, we can infer that the stent's crush resistance increases with reduction in the number of stent crowns in the circumferential direction.

1. Introduction

Our group [Kabinejadian et al. 2013; 2015a; 2015b; Kumar et al. 2016] has been actively developing novel covered stents for preventing small friable parts of atherosclerotic plaques from dislodging into the cerebral blood circulation, and at the same time, preserving external carotid artery (ECA) blood flow. The device comprises of a bare metal stent coated with a biocompatible polymer membrane which has several arrays of cut slits. The main purpose of the slits on the covered membrane was to let blood through the membrane into ECA while confining the plaques along vessel wall and prevent them from dislodging. In one of our earlier in-vitro investigations [Kabinejadian et al. 2015a] we showed that our covered stent design is more efficient in emboli prevention than its corresponding bare metal stent, and at the same time, preserves more than 83% of the original flow of the ECA in carotid artery bifurcation models. Our group evaluated this covered stent design [Kabinejadian et al. 2013; 2015b] (with slit openings on ePTFE membrane) in various models of arteries with different arterial diameters, curvatures, and side-branch angles. We aimed to design new bare metal stents with bigger cell size which can provide higher ECA flow rates through enhanced perfusion to the side-branch as they can accommodate higher number of slits. Larger stent cell size thereby contributes to enhanced slit distribution on the membrane (and

Keywords: stent crown, nitinol, membrane, carotid, stent crush resistance finite element analysis.

thereby better side-branch flow preservation) and desirable crimpability [Kumar and Cui 2016; Kumar et al. 2014]. As part of our stent design-iteration process, we reduced the number of crowns of our open-cell stents in the circumferential direction to get bigger cells and put them through finite element analysis (FEA) to evaluate their crush resistance. Crush resistance can be defined as the ability of a stent to withstand crush loading and therefore prevention of stent collapse is crucial for stent development especially for superficial locations like carotid arteries [García et al. 2012; Timaran et al. 2011; Duerig and Wholey 2002] and peripheral indications as per Food and Drug Administration (FDA) standards [Dhruva et al. 2009; US Food and Drug Administration 2010]. The aim of this study is to evaluate the effect of the number of stent crowns in the circumferential direction on the stent crush resistance through the following steps: (a) analysis of this effect by FEA based modeling and simulation for three different stent designs; (b) fabrication of the stent designs followed by experimental compression tests; (c) providing some explanations with simplified analytical study.

2. Materials & methods

2.1. ***Stent design.*** In this study we took reference from the commercial stent E-Luminexx® stent (Bard Peripheral Vascular Inc., Tempe, AZ) to model the stent which has 12 crowns in the circumferential direction. Additionally, we designed two more stents by reducing their crown numbers to 9 and 6, respectively in the circumferential direction. Figure 1 shows the models of all the three stents. SOLIDWORKS (Dassault Systemes, MA) was used to model the stent geometries and ABAQUS (Dassault Systemes, MA) to conduct FEA. The stents had an outer diameter of 6 mm, a length of 40 mm and struts with uniform thickness of 0.15 mm. These are hybrid stents with combined [Timaran et al. 2011] open- and closed-cell sections (Figure 3). The open-cell sections improve flexibility and enhance stent-vessel conformability without injuring the vessel [Pierce et al. 2009; Carnelli et al. 2011; Tadros et al. 2012]. The closed-cell sections provide sufficient radial strength and in the case of lesions, to secure plaques and hold the plaque in position [Tadros et al. 2012; Hart et al. 2006; Bosiers et al. 2007]. The specifications of stent models considered in this study are given in Table 1. All the three stents were laser-cut from a nitinol tubes of 2.0 mm outer diameter (OD) and 0.18 mm thickness. They were then expanded and shape set using a cylindrical mandrel to 6 mm $\times$ 40 mm (OD $\times$ length) following which electropolishing was done to get a final strut thickness of 0.15 mm. The fabricated nitinol stents for testing are shown in Figure 4.

2.2. ***Material model.*** Nitinol has been used as a stent material as it possesses excellent properties like superelasticity, shape memory, corrosion resistance, biocompatibility, radiopacity, and fatigue resistance [Hansen 2008; Duerig et al. 1999]. When cooled to a very low temperature, nitinol transforms fully to martensite and becomes easily deformable and hence can be effortlessly crimped into a small catheter. When the stent is released into the artery, it recovers to its predetermined, original diameter when exposed to the body temperature which is higher than the Austenite finish (Af) temperature. The built-in Nitinol UMAT was used for our stent simulations. In this model [Auricchio and Taylor 1997; Auricchio et al. 1997] the total strain is the sum of the elastic, transformation and the plastic strain. The mechanical properties of nitinol used in this work are partly from our previous work [Kumar et al. 2013; 2014] and partly based on the information given by our stent fabrication partner and are shown in Table 2.

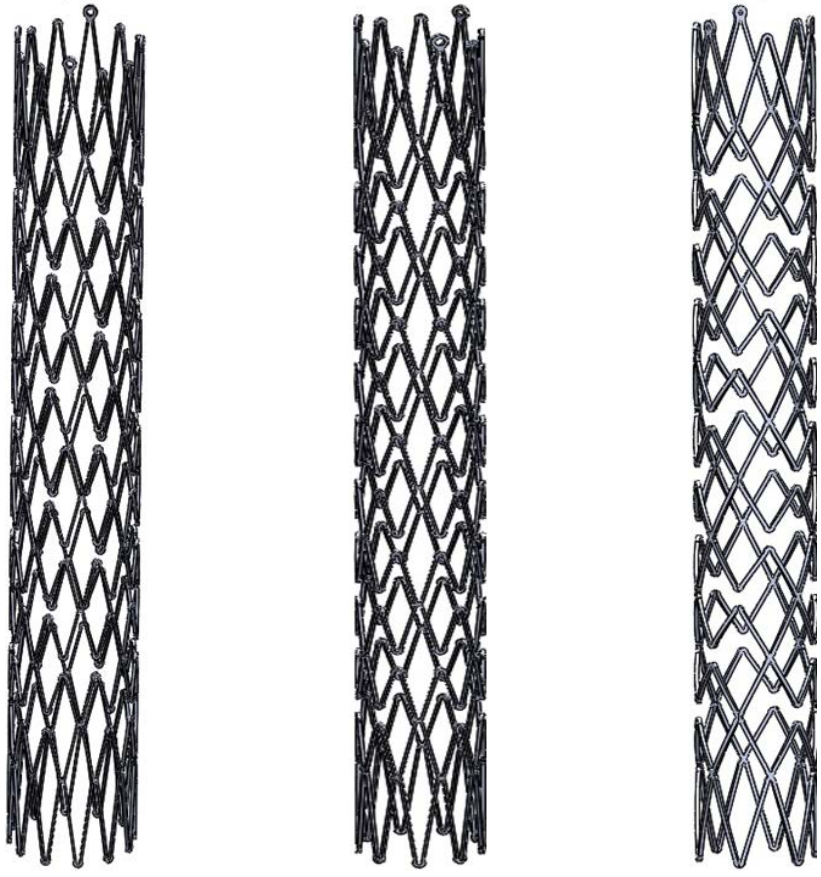

Figure 1. Stent designs investigated in the study: 12 crown design (left), 9 crown design (middle) and 6 crown design (right).

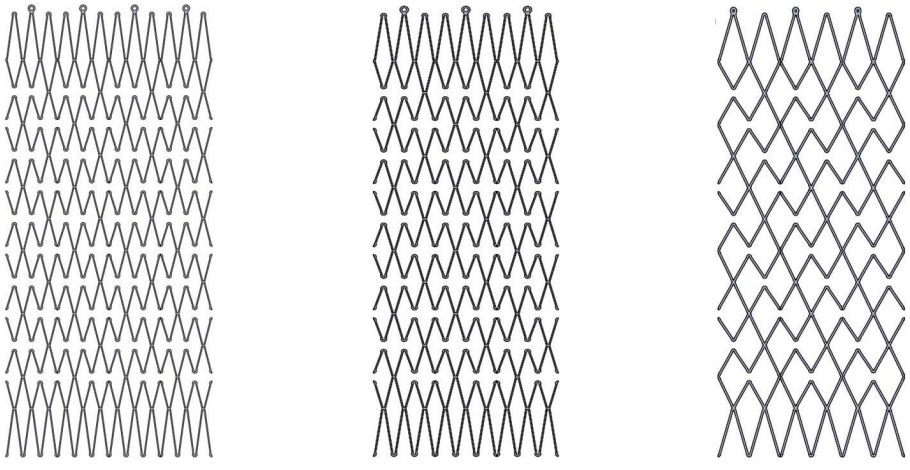

Figure 2. Stent designs with different crown numbers shown in their planar form: 12 crown design (left), 9 crown design (middle) and 6 crown design (right).

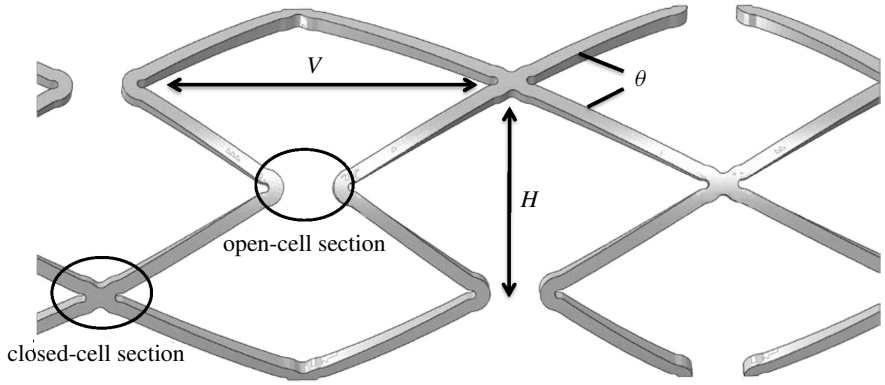

Figure 3. Representation of the stent cell specifications of the stents used in this work (V stands for the distance in axial direction, H the distance in circumferential direction and θ the inter-strut angle).

Figure 4. The three fabricated stents with varying crown numbers in the circumferential direction: 12 crown design (left), 9 crown design (middle) and 6 crown design (right).

stent	12 crown design	9 crown design	6 crown design
outer diameter, OD (mm)	6	6	6
length (mm)	40	40	40
number of crowns	12	9	6
vertical inter-strut distance, V (mm)	5	5	5
inter-crown distance, H (mm)	1.5	2.25	3
inter-strut angle, θ (degree)	21	33	45
strut thickness (mm)	0.15	0.15	0.15
strut width (mm)	0.15	0.15	0.15

Table 1. Specifications of stent models considered in this study.

variables	nitinol
Austenite elasticity, E_{A} (MPa)	40000
Austenite Poisson's ratio, ν_{A}	0.33
Martensite elasticity, E_{M} (MPa)	32000
Martensite Poisson's ratio, ν_{M}	0.33
transformation strain, ε^{l}	0.041
loading $(\delta\sigma/\delta T)_{\mathrm{l}}$ (MPa T^{-1})	6.7
start of transformation loading, $\sigma_{\mathrm{l}}^{\mathrm{s}}$ (MPa)	465
end of transformation loading, $\sigma_{\mathrm{l}}^{\mathrm{e}}$ (MPa)	480
reference temperature, T_0 (°C)	22
unloading, $(\delta\sigma/\delta T)_{\mathrm{u}}$	6.7
start of transformation unloading, $\sigma_{\mathrm{u}}^{\mathrm{s}}$ (MPa)	260
end of transformation unloading, $\sigma_{\mathrm{u}}^{\mathrm{e}}$ (MPa)	248
start of transformation stress in compression, $\sigma_{\mathrm{cl}}^{\mathrm{s}}$ (MPa)	−449
volumetric transformation strain, $\varepsilon_{\mathrm{v}}^{\mathrm{l}}$	0.041
Af temperature (°C)	37
strain limit, $\varepsilon_{\max}$	10%

Table 2. Nitinol material properties.

2.3. ***Computational simulation.*** The ABAQUS/Standard (v. 2017) FEA package was used to carry out the nonlinear FE analysis. The stents were modeled with eight-node linear brick elements with reduced integration and hourglass control. To make sure all the results were independent of further mesh refinements, mesh sensitivity studies were conducted. Mesh convergence was achieved by sequentially increasing the number of elements until there was no appreciable difference in the stress at the end of the analysis. The final mesh of the 6 crown, 9 crown and 12 crown stents comprised of 43,373, 72,481 and 103,845 elements, respectively. For the flat plate compression test, similar to an earlier work [García et al. 2012], each stent was placed between two rigid plates separated by a distance of 6.5 mm. The stents were then compressed by imposing a displacement of 3 mm to the upper plate, similar to the experimental test (described in Section 2.4), while constraining the lower plate in all degrees of freedom

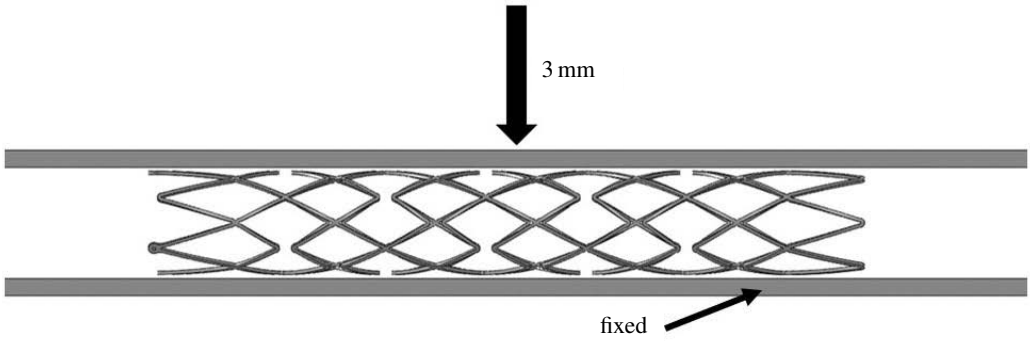

Figure 5. Boundary conditions used in the simulation for radial compression. The lower plate if fixed in to prevent rigid body translation in all three directions.

(see Figure 5). Contact between the plates and the stents was modeled with frictionless tangential and hard normal contact. A penalty interaction property was used to enforce impermeable boundaries. The reaction force after full loading was recorded.

2.4. ***Experimental setup.*** All tests were performed using an Instron 3345 machine (Instron, 825 University Avenue, Norwood, MA 02062, USA) at 20 °C–22 °C. For radial compression test which is similar to the experimental test [Petrini et al. 2005] developed to estimate the radial force of stents, the loads were applied over the full length of the stents with a plate 50 mm in diameter. All stents were placed between two flat plates. No external supports were used for the stents. Three samples were tested for each design (6, 9 and 12 crowns). For the individual stents, the test was repeated three times rotating the stent twice by 120° to negate the possible influence of the rotational orientation of stent. A displacement rate of 20 mm/min was used to start the test until a displacement of 3 mm was achieved. The force and displacement data were recorded using the Instron Bluehill 3 modular applications software for both loading and unloading processes. The experimental setup for the radial compression test is shown in Figure 6.

3. Results

3.1. ***Simulation.*** The results obtained from simulation for the three flat plate compression tests are presented in Figure 7. The results show that the force required to produce a displacement of 3 mm increases with a reduction in the number of crowns. These forces are 5.13 N, 1.03 N and 0.77 N for 6 crown, 9 crown and 12 crown stents, respectively. From the results it can be inferred that the 6 crown stent shows higher crush resistance among the three designs in comparison to the other designs whose crown number increases.

3.2. ***Experiment.*** Response to experimental compression tests is presented in Figure 8. The curves in the experimental results plots represent the mean of the three individual test data for each design. From the experiment, it is evident that the crush resistance of the 6 crown stent is the highest followed by the 9 crown and 12 crown stents. This trend is in agreement with the inference from our simulation results.

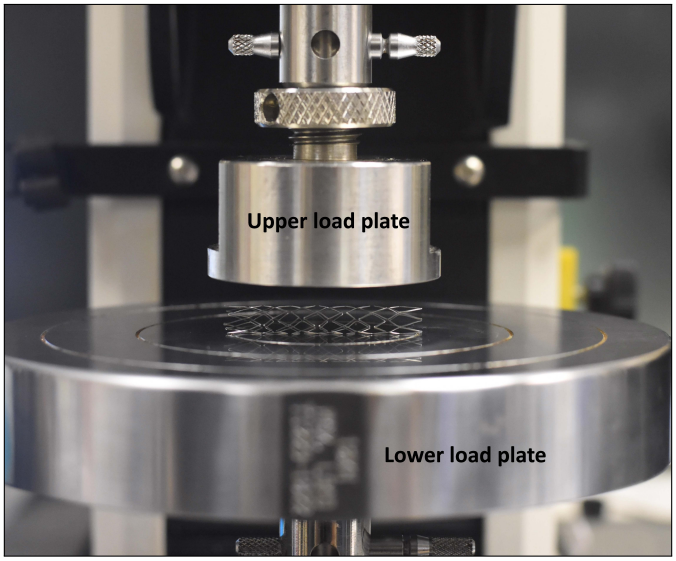

Figure 6. Experimental setup for radial compression test.

4. Discussion

From the simulation and experimental results it could be inferred that even though the metal density reduces as the crown number is reduced in the circumferential direction, surprisingly and contrary to the common observation, the crush resistance of stents increases. There could be a couple of reasons for this

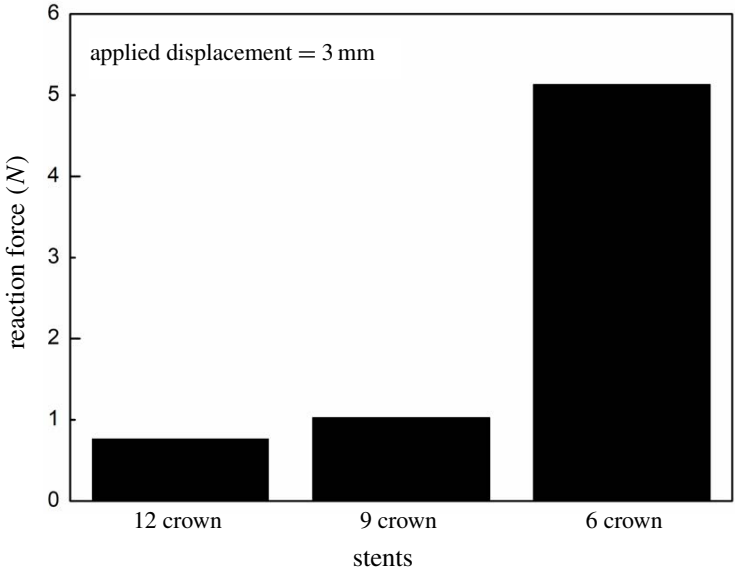

Figure 7. Results of the FEA study: 6 crown stent having maximum reaction force among the three designs in agreement with our experimental results.

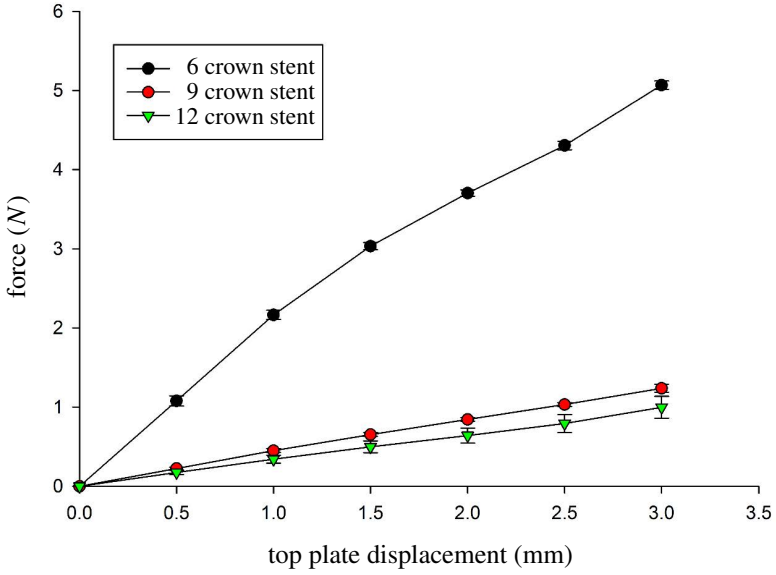

Figure 8. Results of the Experimental study. Force-displacement curve for the radial compression loading of the three stents.

trend. Firstly, when the number of crowns keeps getting reduced in the circumferential direction, there is also a proportional reduction in the open-cell sections which causes the stent to have high stiffness [Carnelli et al. 2011; Moore 2012; Hijazi et al. 2013] as open-cells offer lower stiffness. Secondly, the relationship between crown angle and the crush resistance contributing to the above trend has been explored below in details.

Each stent cell is made up of three basic elements: strut, link, and crown [Alaimo et al. 2017] responsible for crush resistance and crimpability. To understand the increase in the crush resistance with a reduction in the number of crowns, we can consider the stent crown as a simple ring as shown in Figure 9. The zoomed-in part shows one-half of the crown that is considered as a simple beam for the below analytical model.

Let H be the ring height, L the total length, n the number of rings, $\theta = (\text{crown angle})/2$. To obtain the stiffness, a force F is applied at two ends and thereby we have

$$\Delta D = \sum_{i=1}^{2n} \frac{F \cdot \cos\theta}{k_b} \cdot \cos\theta = \frac{F}{k_b} 2n \cos^2\theta, \tag{1}$$

where ΔD is the total displacement in the direction of the force F, and k_b is the beam stiffness. We can write the beam stiffness as

$$k_b = \frac{3EI}{l^3} = \frac{3EI}{(H/\cos\theta)^3},$$

where EI is the bending rigidity of stent strut. Thus the total stiffness k_{total} is

$$k_{\text{total}} = F/\Delta D = C(\cos\theta/n), \tag{2}$$

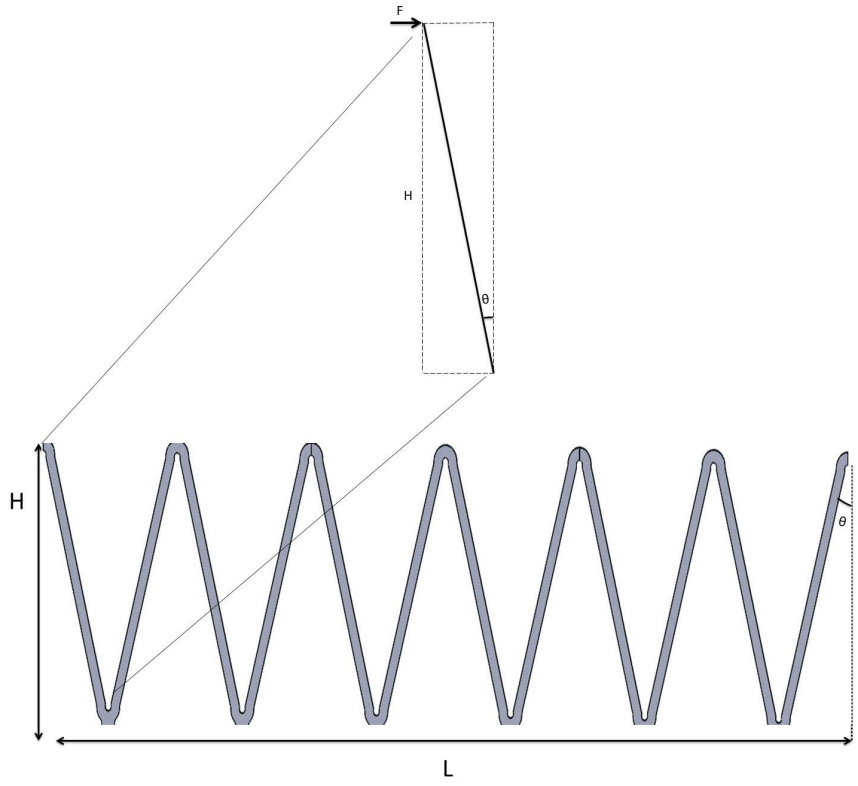

Figure 9. Stent cells being considered as a simple ring to study its stiffness behavior in relation to the number of crowns.

where $C = 3EI/2H^3$. The stiffness can be further expressed as

$$k_{\text{total}} = C \cdot \frac{1}{\sqrt{1 + (L/2nH)^2}} \cdot \frac{1}{n} = C \frac{1}{\sqrt{n^2 + L^2/4H^2}}. \tag{3}$$

Equation (3) shows that when the number of crowns increases, the crush resistance decreases due to a reduction in the total stiffness. When the number of crowns increases, the deformation per crown decreases for a given deformation, thus the load to produce the given total deformation reduces as illustrated in (3). The value of k_{total} as a function of n is plotted in Figure 10, which directly illustrates the relationship between the total stiffness (which determines the crush resistance) and the number of crowns.

5. Conclusion

In this paper the effect of number of crowns on the crush resistance of open-cell stents was studied using FEA and validated through experiment and analytical model. The conclusion made from the study is that the number of crowns in the circumferential direction was inversely proportional to crush resistance of open-cell stents. This is of particular importance especially when stents are designed for superficial locations like the carotid artery where high crush resistance is desirable due to the possibility of the application of external loads. So designing stents with lesser number of open-cells will render

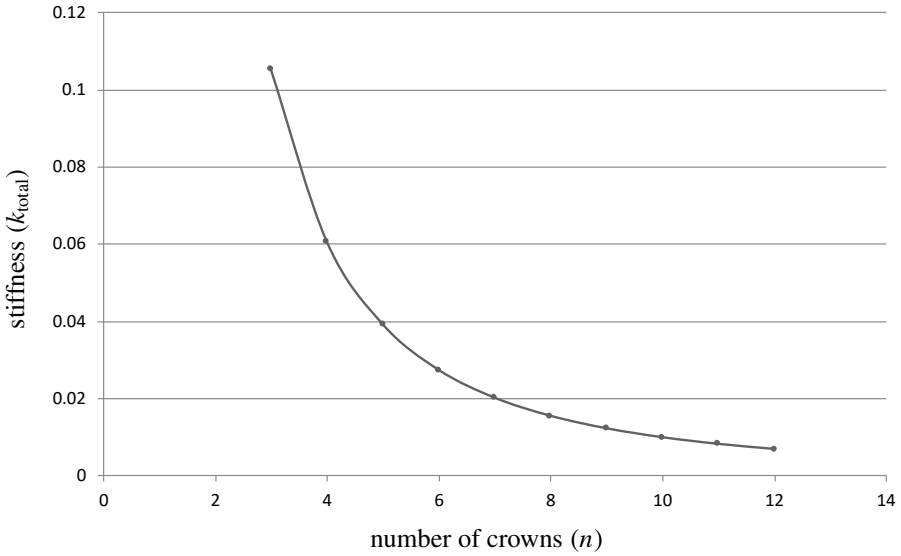

Figure 10. Total stiffness vs number of crowns with the value of k_{total} as a function of n according to (3).

them suitable for application in superficial blood vessels. This work will provide a guideline for stent design in different applications, especially at superficial locations such as carotid and femoral arteries and peripheral indications as per FDA standards where the stents are usually subjected to external loadings during the human activities of daily living.

Acknowledgements

This research is supported by the Singapore Ministry of Health's National Medical Research Council under its Clinician Scientist – Individual Research Grant (CS-IRG) Program (grant number NMRC/CIRG/1385/2014), A*STAR's BEP Program (SERC grant number 141 148 0016) and Singapore-China Joint Research Programme (grant number 1610500025).

References

[Alaimo et al. 2017] G. Alaimo, F. Auricchio, M. Conti, and M. Zingales, "Multi-objective optimization of nitinol stent design", *Med. Eng. Phys.* **47** (2017), 13–24.

[Auricchio and Taylor 1997] F. Auricchio and R. L. Taylor, "Shape-memory alloys: modelling and numerical simulations of the finite-strain superelastic behavior", *Comput. Methods Appl. Mech. Eng.* **143**:1-2 (1997), 175–194.

[Auricchio et al. 1997] F. Auricchio, R. L. Taylor, and J. Lubliner, "Shape-memory alloys: macromodelling and numerical simulations of the superelastic behavior", *Comput. Methods Appl. Mech. Eng.* **146**:3-4 (1997), 281–312.

[Bosiers et al. 2007] M. Bosiers, G. de Donato, K. Deloose, J. Verbist, P. Peeters, F. Castriota, A. Cremonesi, and C. Setacci, "Does free cell area influence the outcome in carotid artery stenting?", *Eur. J. Vasc. Endovasc. Surg.* **33**:2 (2007), 135–141.

[Carnelli et al. 2011] D. Carnelli, G. Pennati, T. Villa, L. Baglioni, B. Reimers, and F. Migliavacca, "Mechanical properties of open-cell, self-expandable shape memory alloy carotid stents", *Artif. Organs* **35**:1 (2011), 74–80.

[Dhruva et al. 2009] S. S. Dhruva, L. A. Bero, and R. F. Redberg, "Strength of study evidence examined by the FDA in premarket approval of cardiovascular devices", *JAMA* **302**:24 (2009), 2679–2685.

[Duerig and Wholey 2002] T. W. Duerig and M. Wholey, "A comparison of balloon- and self-expanding stents", *Minimal. Invasiv. Thera. All. Technol.* **11**:4 (2002), 173–178.

[Duerig et al. 1999] T. Duerig, A. Pelton, and D. Stöckel, "An overview of nitinol medical applications", *Mater. Sci. Eng. A* **273-275** (1999), 149–160.

[García et al. 2012] A. García, E. Peña, and M. Martínez, "Influence of geometrical parameters on radial force during self-expanding stent deployment. Application for a variable radial stiffness stent", *J. Mech. Behav. Biomed. Mater.* **10** (2012), 166–175.

[Hansen 2008] D. C. Hansen, "Metal corrosion in the human body: the ultimate bio-corrosion scenario", *Interface* **17** (2008), 31–34.

[Hart et al. 2006] J. P. Hart, P. Peeters, J. Verbist, K. Deloose, and M. Bosiers, "Do device characteristics impact outcome in carotid artery stenting?", *J. Vasc. Surg.* **44**:4 (2006), 725–730.

[Hijazi et al. 2013] Z. M. Hijazi, T. Feldman, J. Cheatham, and H. Sievert (editors), *Complications during percutaneous interventions for congenital and structural heart disease*, CRC Press, 2013.

[Kabinejadian et al. 2013] F. Kabinejadian, F. Cui, Z. Zhang, P. Ho, and H. L. Leo, "A novel carotid covered stent design: *in vitro* evaluation of performance and influence on the blood flow regime at the carotid artery bifurcation", *Ann. Biomed. Eng.* **41**:9 (2013), 1990–2002.

[Kabinejadian et al. 2015a] F. Kabinejadian, F. Cui, B. Su, A. Danpinid, P. Ho, and H. L. Leo, "Effects of a carotid covered stent with a novel membrane design on the blood flow regime and hemodynamic parameters distribution at the carotid artery bifurcation", *Med. Biol. Eng. Comput.* **53**:2 (2015), 165–177.

[Kabinejadian et al. 2015b] F. Kabinejadian, M. Kaabi Nezhadian, F. Cui, P. Ho, and H. L. Leo, "Covered stent membrane design for treatment of atheroembolic disease at carotid artery bifurcation and prevention of thromboembolic stroke: an in vitro experimental study", *Artif. Organs* **40**:2 (2015), 159–168.

[Kumar and Cui 2016] G. P. Kumar and F. Cui, "Stent design parameters and crimpability", *Int. J. Cardiol.* **223** (2016), 552–553.

[Kumar et al. 2013] G. P. Kumar, F. Cui, A. Danpinid, B. Su, J. K. F. Hon, and H. L. Leo, "Design and finite element-based fatigue prediction of a new self-expandable percutaneous mitral valve stent", *Comput.-Aided Des.* **45**:10 (2013), 1153–1158.

[Kumar et al. 2014] G. P. Kumar, F. Cui, H. Q. Phang, B. Su, H. L. Leo, and J. K. F. Hon, "Design considerations and quantitative assessment for the development of percutaneous mitral valve stent", *Med. Eng. Phys.* **36**:7 (2014), 882–888.

[Kumar et al. 2016] G. P. Kumar, F. Kabinejadian, J. Liu, P. Ho, H. L. Leo, and F. Cui, "Simulated bench testing to evaluate the mechanical performance of new carotid stents", *Artif. Organs* **41**:3 (2016), 267–272.

[Moore 2012] W. S. Moore, *Vascular and endovascular surgery: a comprehensive review expert consult*, Elsevier Health Sciences, 2012.

[Petrini et al. 2005] L. Petrini, F. Migliavacca, P. Massarotti, S. Schievano, G. Dubini, and F. Auricchio, "Computational studies of shape memory alloy behavior in biomedical applications", *J. Biomech. Eng.* (*ASME*) **127**:4 (2005), 716–725.

[Pierce et al. 2009] D. S. Pierce, E. B. Rosero, J. G. Modrall, B. Adams-Huet, R. J. Valentine, G. P. Clagett, and C. H. Timaran, "Open-cell versus closed-cell stent design differences in blood flow velocities after carotid stenting", *J. Vasc. Surg.* **49**:3 (2009), 602–606.

[Tadros et al. 2012] R. O. Tadros, C. T. Spyris, A. G. Vouyouka, C. Chung, P. Krishnan, M. W. Arnold, M. L. Marin, and P. L. Faries, "Comparing the embolic potential of open and closed cell stents during carotid angioplasty and stenting", *J. Vasc. Surg.* **56**:1 (2012), 89–95.

[Timaran et al. 2011] C. H. Timaran, E. B. Rosero, A. Higuera, A. Ilarraza, J. G. Modrall, and G. P. Clagett, "Randomized clinical trial of open-cell vs closed-cell stents for carotid stenting and effects of stent design on cerebral embolization", *J. Vasc. Surg.* **54**:5 (2011), 1310–1316.e1.

[US Food and Drug Administration 2010] US Food and Drug Administration, "Non-clinical engineering tests and recommended labeling for intravascular stents and associated delivery systems", Guidance for industry and FDA staff, U.S. Department of Health and Human Services, 2010, Available at https://www.fda.gov/media/71639/download.

Received 11 Jun 2019. Revised 16 Dec 2019. Accepted 20 Dec 2019.

GIDEON PRAVEEN KUMAR: vijayagpk@ihpc.a-star.edu.sg
Institute of High Performance Computing, Singapore 138632, Singapore

KEPING ZUO: keping.zuo@gmail.com
National University of Singapore, Singapore 119077, Singapore

LI BUAY KOH: maykoh88@gmail.com
National University of Singapore, Singapore 119077, Singapore

CHI WEI ONG: bieocw@nus.edu.sg
National University of Singapore, Singapore 119077, Singapore

YUCHENG ZHONG: zhong_yucheng@ihpc.a-star.edu.sg
Institute of High Performance Computing, Singapore 138632, Singapore

HWA LIANG LEO: bielhl@nus.edu.sg
National University of Singapore, Singapore 119077, Singapore

PEI HO: pei_ho@nuhs.edu.sg
National University of Singapore, Singapore 119077, Singapore

FANGSEN CUI: cuifs@ihpc.a-star.edu.sg
Institute of High Performance Computing, Singapore 138632, Singapore

JOURNAL OF MECHANICS OF MATERIALS AND STRUCTURES

msp.org/jomms

Founded by Charles R. Steele and Marie-Louise Steele

Cover photo: Ev Shafrir

See msp.org/jomms for submission guidelines.

JoMMS (ISSN 1559-3959) at Mathematical Sciences Publishers, 798 Evans Hall #6840, c/o University of California, Berkeley, CA 94720-3840, is published in 10 issues a year. The subscription price for 2020 is US $660/year for the electronic version, and $830/year (+$60, if shipping outside the US) for print and electronic. Subscriptions, requests for back issues, and changes of address should be sent to MSP.

JoMMS peer-review and production is managed by EditFLOW® from Mathematical Sciences Publishers.

PUBLISHED BY

mathematical sciences publishers

nonprofit scientific publishing

http://msp.org/

Journal of Mechanics of Materials and Structures

Volume 15, No. 1 January 2020

Stress-minimizing holes with a given surface roughness in a remotely loaded elastic plane SHMUEL VIGDERGAUZ and ISAAC ELISHAKOFF 1

Analytical modeling and computational analysis on topological properties of 1-D phononic crystals in elastic media MUHAMMAD and C. W. LIM 15

Dynamics and stability analysis of an axially moving beam in axial flow YAN HAO, HULIANG DAI, NI QIAO, KUN ZHOU and LIN WANG 37

An approximate formula of first peak frequency of ellipticity of Rayleigh surface waves in an orthotropic layered half-space model TRUONG THI THUY DUNG, TRAN THANH TUAN, PHAM CHI VINH and GIANG KIEN TRUNG 61

Effect of number of crowns on the crush resistance in open-cell stent design GIDEON PRAVEEN KUMAR, KEPING ZUO, LI BUAY KOH, CHI WEI ONG, YUCHENG ZHONG, HWA LIANG LEO, PEI HO and FANGSEN CUI 75

A dielectric breakdown model for an interface crack in a piezoelectric bimaterial YURI LAPUSTA, ALLA SHEVELEVA, FRÉDÉRIC CHAPELLE and VOLODYMYR LOBODA 87

Thermal buckling and free vibration of Timoshenko FG nanobeams based on the higher-order nonlocal strain gradient theory GORAN JANEVSKI, IVAN PAVLOVIĆ and NIKOLA DESPENIĆ 107

A new analytical approach for solving equations of elasto-hydrodynamics in quasicrystals VALERY YAKHNO 135

Expansion-contraction behavior of a pressurized porohyperelastic spherical shell due to fluid redistribution in the structure wall VAHID ZAMANI and THOMAS J. PENCE 159

1559-3959(2020)15:1;1-L